Reversible Oxidation Quantified by Optical Properties in Epitaxial $Fe_2CrO_{4+\delta}$ Films on (001) $MgAl_2O_4$

Mark D. Scafetta,[1#] Tiffany C. Kaspar,[1] Mark E. Bowden,[2] Steven R. Spurgeon,[3] Bethany Matthews,[3] Scott A. Chambers[1]*

1) Physical and Computational Sciences Directorate, Pacific Northwest National Laboratory, Richland, WA, USA;

2) Environmental Molecular Sciences Laboratory, Pacific Northwest National Laboratory, Richland, WA, USA;

3) Energy and Environment Directorate, Pacific Northwest National Laboratory, Richland, WA, USA

#Present address: Department of Environmental Simulations, Air Force Tactical Center, Patrick Air Force Base, FL, USA

SUPPLEMENTAL:

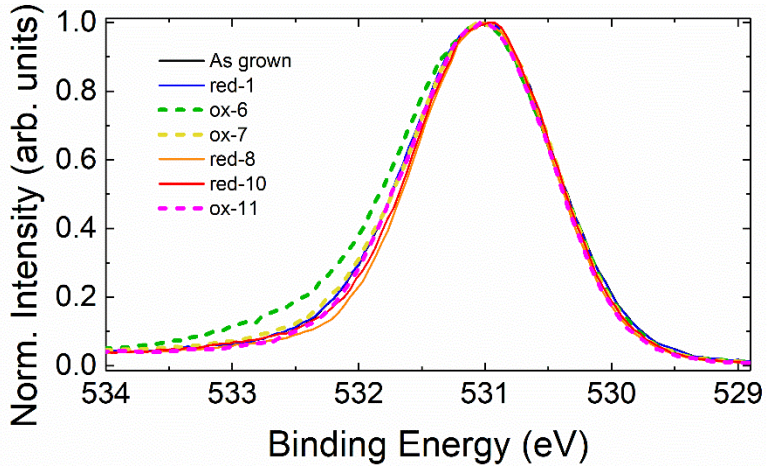

Figure S1. O 1*s* XPS spectra for various anneals. Thick dashed lines represent oxidizing anneals relative to the sample in its previous condition. Thin solid lines represent the as-grown and reducing anneals relative to the sample in its previous condition.

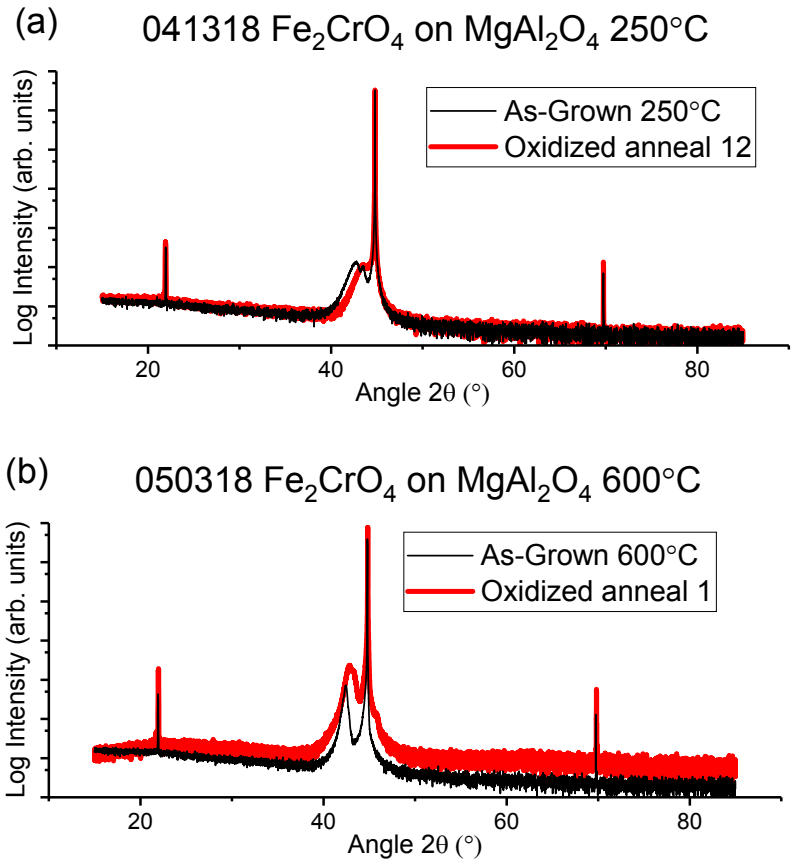

Figure S2. Out-of-plane XRD for films deposited at (a) 250 °C and at (b) 600 °C, before and after annealing. The observed difference in background for the annealed and as-grown film at 600 °C results from the use of a different diffractometer.

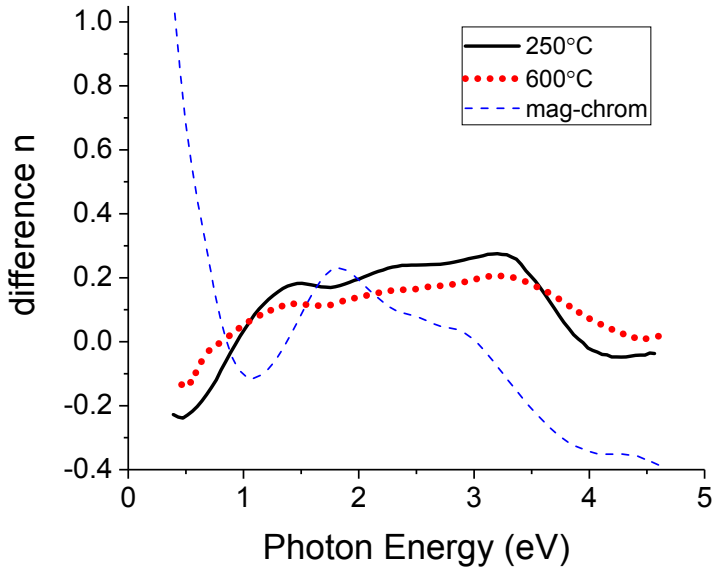

Figure S3. Difference between the refractive index (*n*) for the most oxidized sample and the least oxidized sample. The dashed thin line is for magnetite minus chromite.

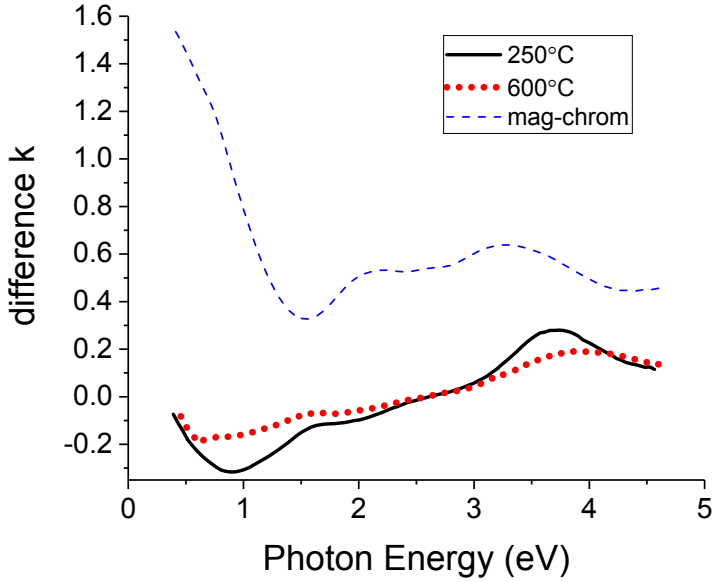

Figure S4. Difference between the extinction coefficient (*k*) for the most oxidized sample and the least oxidized sample. The dashed thin line is for magnetite minus chromite.

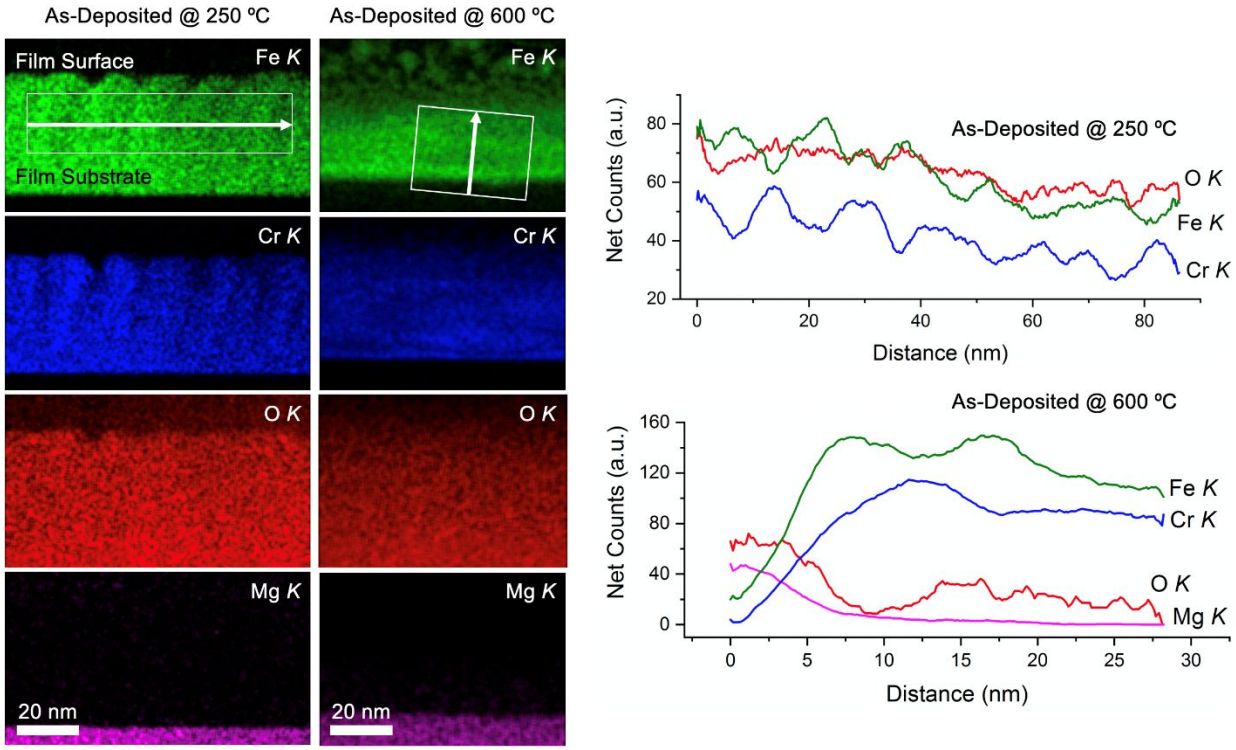

Figure S5. Corresponding STEM-EDS maps for the as-grown films deposited at 250 °C (left) and 600 °C (right), respectively. Chemical segregation behavior is observed independent of the deposition temperature, as shown in the EDS line scans in the respective panels on the right. The line scan direction is highlighted by the white arrows on the respective panels on the left. Cation segregation is perpendicular or parallel to the

film-substrate interface at 250 °C or 600 °C, respectively. Redeposition from sample preparation can be observed in the Pt coating for sample deposited at 600 °C.

The Cr-to-Fe ratio at the surface changes upon oxidation as measured by XPS and as shown in Figures 1(d) and S7. This change does not have an obvious effect on XRR which makes its detection difficult or possibly unrealistic via ellipsometry analysis alone. To determine if the different cation segregation behavior measured before and after annealing causes a significant difference in optical properties, we introduced a surface layer into our model. For instance, we used the optical data collected from the as-grown film deposited at 250 °C.

The WVASE fitting software yields unrealistic results when the two-layer model is used to fit both layers independently. Therefore, to observe the effect of cation segregated surface layers, we used a two-layer model by fixing the optical properties of the surface layer (top 3 nm) to that of magnetite or chromite. These surface layer compositions are

the most extreme scenarios and are unrealistic based on the STEM and XPS data. We observed a <15% difference in cation stoichiometry across the different domains according to STEM-EDS, and <11% difference measured in surface cation stoichiometry from XPS, before and after oxidizing anneals. But using these extremes should yield the largest difference and signal the possible difference in optical properties in the thickest region of the film resulting from such a scenario. We allowed the optical properties of the layer closest to the substrate (the majority of the film thickness at ~40 nm) to vary. The result of this analysis can be seen in supplemental Figure S6. The optical properties do not significantly vary for the thick layer close to the substrate by modeling the top ~3 nm as magnetite or chromite, especially compared to the changes that occur from oxidation or reduction. While different film layering may exist before and after annealing, the difference does not in all likelihood have a significant effect on the optical properties based on this analysis.

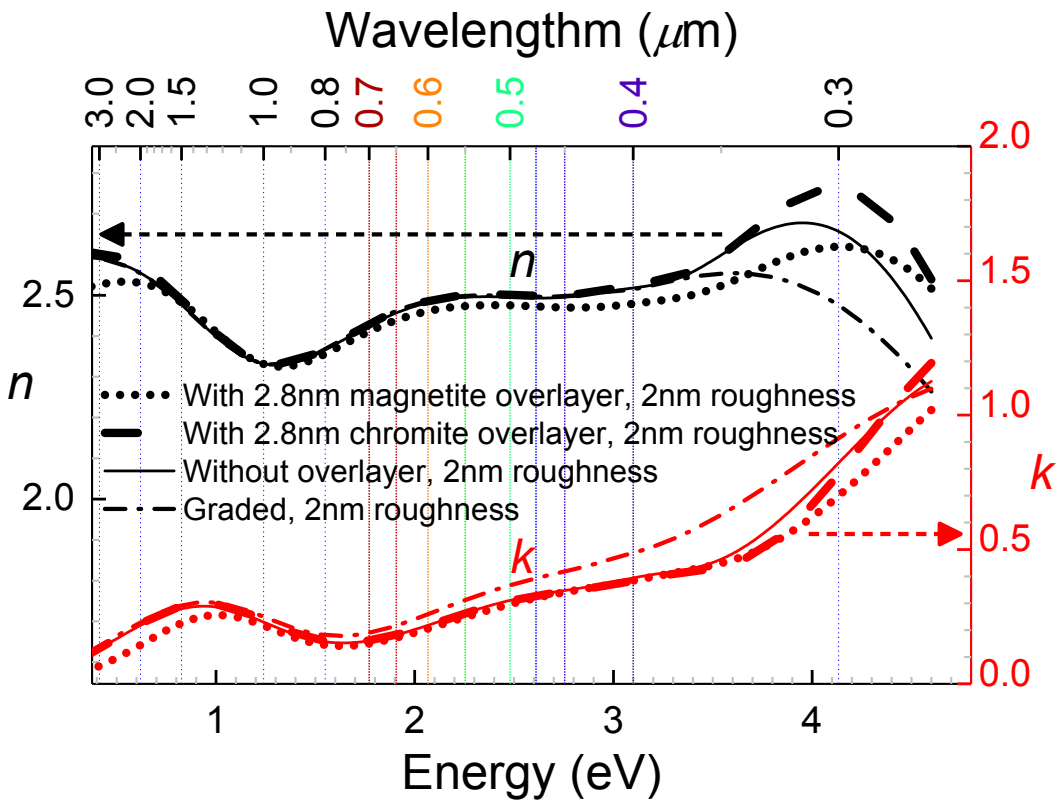

Figure S6. Optical properties of the film deposited at 250 °C modeled without a surface layer (thin solid lines), with a 3 nm magnetite surface layer (dotted lines), with a 3 nm chromite surface layer (dashed lines), and as a graded layer (dashed and dotted lines). All models incorporate 2nm of surface roughness

We also modeled the film as a graded layer in an attempt to induce a larger difference. This result is also shown in supplemental Figure S6. While the graded model does introduce the largest difference from the single homogeneous layer model, this model is the most unrealistic based on XRR data. The result is also not significantly different

compared to the changes observed upon oxidizing/reducing anneals around 0.9 eV. Therefore, we are confident that the observed changes in the optical properties significantly result from changes in the electronic structure induced by changing the Fe valence (δ) in the films.

.

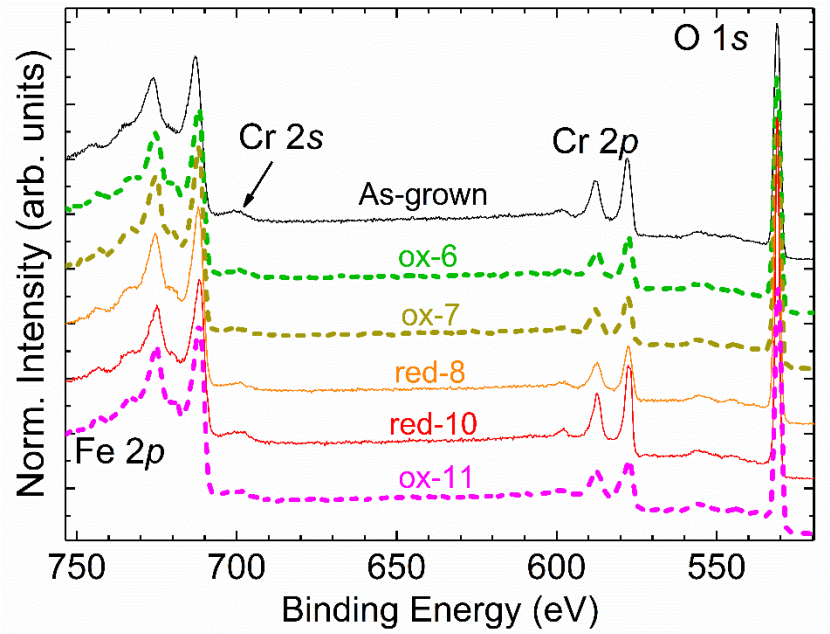

Figure S7. Low-energy-resolution Fe 2*p*, Cr 2*p* and O 1*s* spectra (normalized to constant O 1*s* intensity). Thick dashed lines represent anneals expected to result in increased oxidation compared to the previous condition. Thin solid lines represent as-grown or anneals expected to decrease oxidation compared to the previous condition.

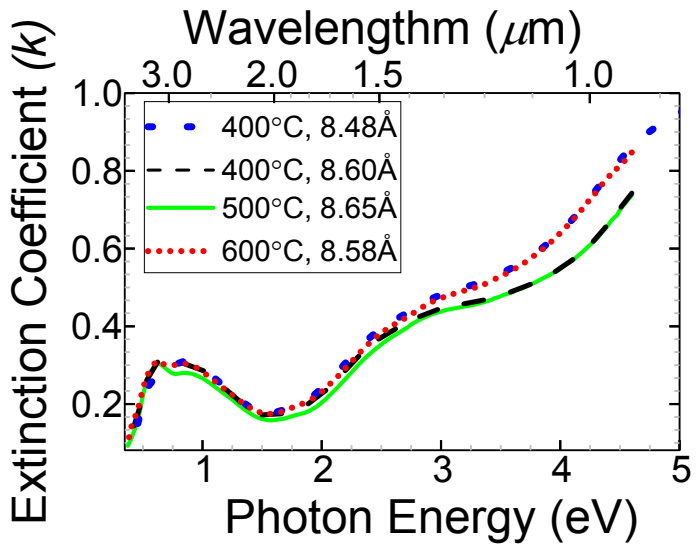

Figure S8. Extinction coefficient (*k*) versus incident photon energy for various Fe_2CrO_4 films, as-deposited on $MgAl_2O_4$ (001). The measurement listed in the legend for each curve is the OOP lattice parameter for the respective film, in the as-deposited state. The only systematic and significant trends are in the low photon energy region which we have previously shown and discussed in reference 4.

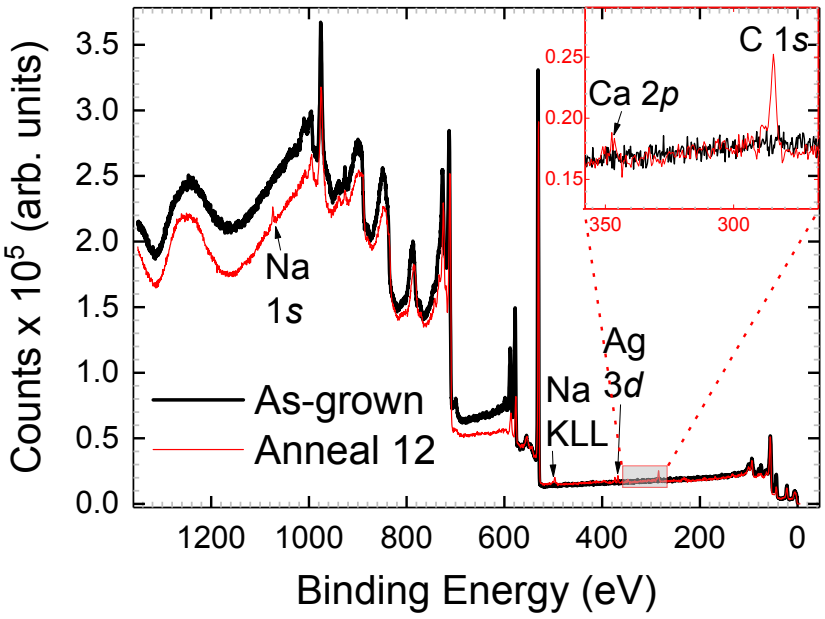

Figure S9. X-ray photoelectron spectra for the film deposited at 250 °C in the as deposited state and after annealing in air at 400 °C for 1hr (ox-12). Several dilute contaminants from the annealing apparatus, sample holder, and sample handling are introduced, but no Mg is observed even after 12 anneals totaling 105 hours. This, along with Figure S8 confirms the insignificance of Mg contamination on the material properties after heat treatment.